Intravenous Glu-plasminogen attenuates cholesterol crystal embolism-induced thrombotic angiopathy, acute kidney injury and

Nephrol Dial Transplant (2023) 38: 93–105
https://doi.org/10.1093/ndt/gfac273
Advance Access publication date 14 September 2022

Intravenous Glu-plasminogen attenuates cholesterol crystal embolism-induced thrombotic angiopathy, acute kidney injury and kidney infarction

Lyuben Lyubenov[1], Chongxu Shi[1], Danyang Zhao[1], Luying Yang[1], Yutian Lei[1], Elmina Mammadova-Bach[1,2], Letizia de Chiara[3,4], Roberto Semeraro[5], Samuela Landini[6], Paola Romagnani[3,4], Elena Vörg[7], Satish K. Devarapu[7], Ricarda Welz[7], Stephan T. Kiessig[7] and Hans-Joachim Anders[1]

[1]Department of Medicine IV, Hospital of Ludwig-Maximilian-University, Munich, Germany, [2]Walther-Straub-Institute for Pharmacology and Toxicology, Ludwig-Maximilian-University, Munich, Germany, [3]Department of Experimental and Biomedical Sciences "Mario Serio", University of Florence, Florence, Italy, [4]Nephrology and Dialysis Unit, Meyer Children's Hospital IRCCS, Florence, Italy, [5]Department of Experimental and Clinical Medicine, University of Florence, Florence, Italy, [6]Medical Genetics Unit, Meyer Children's University Hospital, Florence, Italy and [7]PreviPharma Consulting GmbH, Mannheim, Germany

Correspondence to: Hans-Joachim Anders; E-mail: hjanders@med.uni-muenchen.de; Twitter: @hjanders_hans

GRAPHICAL ABSTRACT

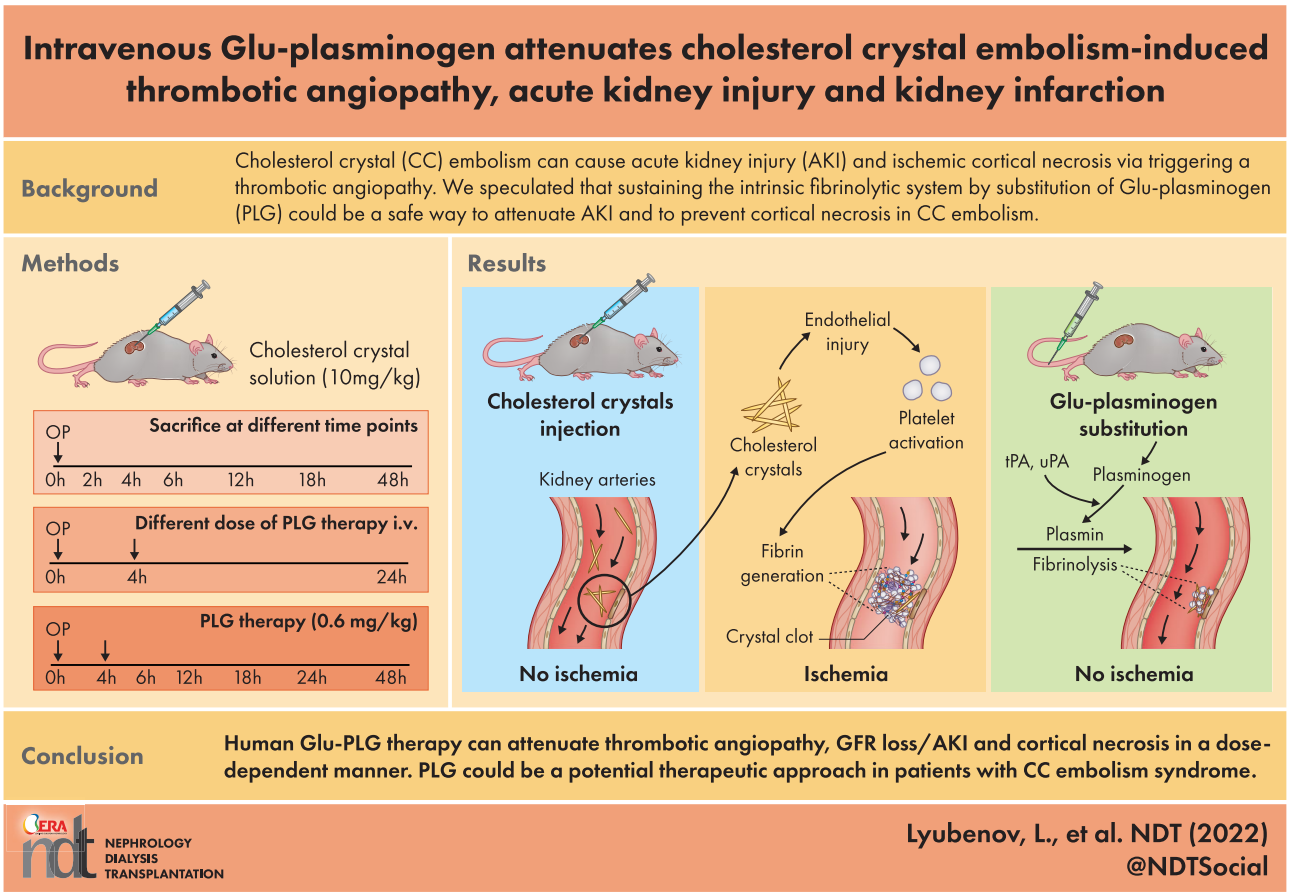

KEY LEARNING POINTS

What is already known about this subject?

- Cholesterol crystal (CC) embolism is a potentially fatal complication of severe atherosclerosis.
- Kidney CC embolism causes acute kidney injury (AKI) by triggering thrombotic angiopathy.
- Fibrinolytic drugs are effective but may cause bleeding complications.

What this study adds?

- We characterize the dynamics of crystal thrombus formation in a mouse model of CC embolism.
- Glu-plasminogen (Glu-Plg) extracts from human plasma injected intravenously 4 h after CC injection into the left kidney artery of mice attenuated thrombotic angiopathy, AKI and cortical necrosis in a dose-dependent manner.
- An intermediate dose had a transient effect, which renders Glu-Plg well-controllable intervention, although no bleeding complications occurred during or after the treatment period.

What impact this may have on practice or policy?

- Glu-Plg might be a potential therapeutic approach in patients with CC embolism syndrome–related AKI.

ABSTRACT

Background. Cholesterol crystal (CC) embolism causes acute kidney injury (AKI) and ischaemic cortical necrosis associated with high mortality. We speculated that sustaining the fibrinolytic system with Glu-plasminogen (Glu-Plg) could be a safe way to attenuate AKI and prevent ischaemic infarction upon CC embolism.

Methods. We induced CC embolism by injecting CC into the left kidney artery of C57BL/6J mice. The primary endpoint was glomerular filtration rate (GFR).

Results. Starting as early as 2 h after CC embolism, thrombotic angiopathy progressed gradually in the interlobular, arcuate and interlobar arteries. This was associated with a decrease of GFR reaching a peak at 18 h, i.e. AKI, and progressive ischaemic kidney necrosis developing between 12–48 h after CC injection. Human plasma Glu-Plg extracts injected intravenously 4 h after CC embolism attenuated thrombotic angiopathy, GFR loss as well as ischaemic necrosis in a dose-dependent manner. No bleeding complications occurred after Glu-Plg injection. Injection of an intermediate dose (0.6 mg/kg) had only a transient protective effect on microvascular occlusions lasting for a few hours without a sustained protective effect on AKI at 18–48 h or cortical necrosis, while 1.5 mg/kg were fully protective. Importantly, no bleeding complications occurred.

Conclusions. These results provide the first experimental evidence that Glu-Plg could be an innovative therapeutic strategy to attenuate thrombotic angiopathy, AKI, kidney necrosis and potentially other clinical manifestations of CC embolism syndrome.

Keywords: atheroembolism, fibrinolysis, renal failure, thrombotic microangiopathy

INTRODUCTION

Atherosclerosis is a leading cause of global morbidity and mortality [1]. Occlusive complications of atherosclerosis include atherothrombosis, atheroembolism and cholesterol crystal (CC) embolism [1–3]. CC embolism occurs at a frequency of 6.2 cases per million population per year and is frequently fatal when affecting several organs [3, 4]. CC embolism is usually the consequence of spontaneous or intervention-related rupture of the fibrous cap of a large atheromatous plaque in the aorta that mobilizes CC and other plaque material into the circulation [3, 5, 6]. Such CC showers end in peripheral arteries and cause ischaemic necrosis of many organs, with the kidney being the primary site followed by skin, gastrointestinal tract and brain [3, 7]. Consequently, clinical manifestations of CC embolization include acute kidney injury (AKI), skin necrosis ('blue toe syndrome') and intestinal and neurological symptoms [3, 8].

Study of the pathophysiology of CC embolism–related AKI and ischaemic cortical necrosis requires a reproducible animal model, e.g. based on injecting a CC suspension into the kidney artery of mice [9]. Injected crystals affect arterial vessels of different dimensions, a process that triggers endothelial injury and immunothrombosis, including the morphological lesion pattern of thrombotic angiopathy [9]. Interestingly, these 'crystal clots' are the primary cause of organ failure and tissue necrosis. Hence the use of anticoagulants can prevent AKI and cortical necrosis, demonstrating that not the crystals *per se* but the crystal clots account for organ failure and necrosis [9]. Indeed, even necrosis inhibitors preventing all cortical necrosis had no effect on glomerular filtration rate (GFR) loss/AKI as long as afferent arterioles remained obstructed by crystal clots [9].

However, the use of anticoagulants in patients with CC embolism syndrome has shown discrepant results [3, 8, 10–12]. In addition, bleeding complications remain a concern when using anticoagulants.

Substitution of several human plasma proteins has been used in critically ill patients to modulate the coagulation cascade or the systemic inflammatory response syndrome [13, 14]. Here we speculated that injection of the native plasminogen (Plg), which contains a glutamic acid residue at the N-terminus, referred to as Glu-Plg, could augment the intrinsic fibrinolytic system to attenuate crystal clot formation [15]. In contrast, Lys-Plg is a minor component of human plasma. Plg is the zymogen form of the fibrinolytic

serine protease plasmin, constitutively expressed by the liver, and circulates in the plasma. Binding to fibrin changes its conformation so that tissue Plg activator (tPA), kallikreins, fibrin and factor XII can trigger plasmin activation [16, 17]. We therefore hypothesized that intravenous human Plg might attenuate thrombotic angiopathy, AKI and ischaemic kidney infarction upon CC embolism.

MATERIALS AND METHODS

Human Glu-Plg preparation and application

The starting material for Glu-Plg purification was obtained from CSL Behring AG (Bern, Switzerland); Glu-Plg was purified and characterized at PreviPharma (Mannheim, Germany). We purified Plg from human cryo-poor plasma by a two-step chromatographic purification approach followed by an affinity-based capture step to isolate Plg. The frozen feed streams were thawed, centrifuged and filtered, followed by a polishing step using strong anion exchange resin Fractogel M TMAE to bind unwanted serine proteases, leaving Plg in the flow-through. In the two human plasma-based runs, at least 90% of the Plg could be detected in the flow-through and only trace amounts in the eluate (10% loss). The flow-through fractions of the polishing steps were used as feeds for lysine affinity chromatography. The two affinity capture runs resulted in comparable yields ranging from 70 to 80%. Analysis of the eluate confirmed the purity of the product by demonstrating the absence of any Lys-Plg/-plasmin form or any other significant protein-related impurities (Supplementary Fig. 1). The eluates were used for the *in vivo* studies. All Plg aliquots were kept at −80°C in an endotoxin-free environment. Plg was injected intravenously into the tail vein of the animals.

Preparation of CC injection solution

A pre-calculated quantity of CC powder (grade ≥99%; Sigma-Aldrich, Steinheim, Germany) was suspended in sterile phosphate-buffered saline to achieve a concentration of 2 mg/ml. The weight of the solution was recorded before and after the addition of CC. Finally, the solution was autoclaved at 120°C and stored at 4°C. The solution was warmed to body temperature shortly before use. In all experiments, the injected concentration of CC was 10 mg/kg.

Animal studies

Seven- to eight-week-old healthy male C57BL/6J mice were obtained from Charles River Laboratories (Sulzfeld, Germany) and housed in groups of five in polypropylene cages under a 12 h light–dark cycle at a room temperature of 22 ± 2°C with unlimited access to food and water. The group size was seven for the non-interventional time course experiment, seven for the different doses of Plg and six for the intermediate Plg dose experiment. Animals were stratified by age and randomized to different treatment groups. Regular animal welfare scoring was performed according to regulations and procedures set by the local animal welfare committee. All experimental procedures were approved by the local government authorities according to the European equivalent of the National Institutes of Health Guide for the Care and Use of Laboratory Animals (directive 2010/63/EU).

Intra-arterial injection of cholesterol crystals

CC injection was performed as described [9]. In brief, mice were anaesthetized by intraperitoneal injection of medetomidine (0.5 mg/kg), midazolam (5 mg/kg) and fentanyl (0.05 mg/kg). To maintain a normal body temperature, mice were kept in a heating chamber during anaesthesia induction and wake-up periods [18]. After shaving and disinfection, the kidney was exposed through a 1 cm left flank incision to expose the kidney artery and inject 10 mg/kg of the freshly vortexed CC suspension via a 33-gauge needle. Upon removal of the needle, blood loss was contained using a haemostatic gelatine sponge at the injection site before closing the wound with absorbable sutures. We reversed the anaesthesia with atipamezole (2.5 mg/kg) and flumazenil (0.5 mg/kg). Regular subcutaneous injections of buprenorphine ensured pain control.

Measured GFR

We measured GFR transcutaneously in conscious and freely moving mice as described previously [9]. In brief, we used a miniaturized imaging device consisting of two light-emitting diodes, a photodiode and a battery (MediBeacon, Mannheim, Germany) that was attached to the skin using double-sided adhesive tape. Mice received an intravenous tail vein injection of fluorescein isothiocyanate–sinistrin (150 mg/kg) tracer (Mannheim Pharma & Diagnostics, Mannheim, Germany) and the signal was recorded for 1.5 h. GFR was calculated using the MPD Lab Software (Mannheim Pharma & Diagnostics) in a model consisting of three compartments, mouse body weight and an empirical conversion factor.

Single-cell RNA sequencing

Wild-type C57Bl/6 mouse kidneys were minced into 1-mm pieces and incubated at 37°C for 10 min in a buffer containing 250 U/ml Liberase (Roche, Mannheim, Germany) and 40 U/ml DNase I (Sigma-Aldrich, Taufkirchen, Germany). The obtained solution was then transferred to a C-tube to twice run the gentle MACS D1 program (Miltenyi Biotec, Bergisch Gladbach, Germany). The reaction was stopped by adding 10% foetal bovine serum and the dissociated cells were passed through a 40-µm cell strainer and incubated with RBC lysis buffer, cleared using a dead cell removal kit (Miltenyi Biotec) and run on a 10× Chromium Single Cell instrument (10× Genomics, Leiden, The Netherlands) at a 95% cell viability. Raw sequencing data were processed using the Cell Ranger pipeline (software version 3.0.1; 10× Genomics). First, Cell Ranger FASTQ demultiplexed libraries based on sample indices converted the barcode and read data to FASTQ files. Second, Cell Ranger count took FASTQ files and performed alignment to the mouse mm10 reference genome [19] and then proceeded with filtering and unique molecular identifier counting. Quality control removed poor-quality cells and

detected genes using a mitochondrial read >40% and <200 genes, respectively. Cell-specific biases were normalized by dividing the measured counts by the size factor obtained through the scran-computed SumFactors method [20]. Finally, all counts were log-transformed after the addition of a pseudocount of 1. We obtained 3766 cells from healthy mouse kidneys. Next we looked for 'informative' genes to use for dimensional reduction through a principal component analysis. The first 50 principal components were used to construct a neighbourhood graph of observations [21] through the pp.neighbours function, which relies on the Uniform Manifold Approximation and Projection (UMAP) algorithm to estimate the connectivity of data points. The data were clustered at resolutions (0.5, 1, 2) by the tl.louvain function.

Histological assessment

Kidneys were harvested for immunostaining using standard protocols [22]. Sections of 2-µm-thick kidney tissue were stained for fibrinogen (ab27913; Abcam, Cambridge, UK) and smooth muscle actin (SMA; M0852; Dako, Jena, Germany) to localize arterial vessels and clots, respectively. Anti-CD31 (DIA-310; Dianova, Hamburg, Germany) was used to determine the approximate percentage of viable endothelial cells in the kidney. A semiquantitative injury score was assessed on periodic acid–Schiff (PAS)-stained sections. Injury criteria included the degree of tubular necrosis, tubular dilation, cast formation, brush border loss and interstitial oedema. Anti-Ly6B (MCA771G; Serotec, Raleigh, NC, USA) was used to identify neutrophil infiltration into the renal parenchyma. Anti-human PLG (SAPG-AP; CoaChrom, Maria Enzersdorf, Austria), anti-mouse PLG (PAB236Mu01; Cloud-Clone, Katy, TX, USA) and anti-tPA (ABIN2855635; Antibodies-online, Limerick, PA, USA) staining were also incorporated into the study. All sections were assessed by a blinded observer.

Statistical analysis

All statistical analyses were performed using GraphPad Prism 8.0 (GraphPad Software, San Diego, CA, USA). Prior to each analysis we assessed the normal distribution of the data (Shapiro–Wilk test), homo- and heteroscedasticity (Levene's test) and the presence of outliers (Grubb's test). Normally distributed and homoscedastic data were tested for statistical significance using a one-way analysis of variance (three or more groups) and *t*-test (two groups). The post hoc Bonferroni test was used for multiple comparisons. Heteroscedastic data were corrected using the Games–Howell post hoc test. Not normally distributed data sets were compared using the Kruskal–Wallis test. *P*-values <.05 were considered statistically significant.

RESULTS

Expression profile of fibrinolytic factors in the kidney

The components of the fibrinolytic system have been characterized in human kidneys [23, 24]. Single-cell RNA sequencing confirmed the absence of Plg messenger RNA expression inside cells of the mouse kidney, while urokinase-type Plg activator is expressed by different kidney cell types (Fig. 1A, Supplementary Fig. 2). tPA showed strong positivity also in the glomeruli (Fig. 1A). Immunostaining for murine Plg was limited to occasional endothelial cells located in the peritubular capillaries (Fig. 1B). In contrast, tPA positivity distributed diffusely across the kidney cortex in tubular epithelial cells and glomerular endothelial cells (Fig. 1C), consistent with the RNA sequencing data. These expression patterns were consistent with an extrarenal source of Plg activated towards plasmin inside the kidney via a locally expressed tPA. Upon intravenous injection into healthy mice, human Plg localized to endothelial cells of peritubular vascular endothelial cells (Fig. 1D). When human Plg was injected into mice 4 h after CC embolism, immunostaining for human Plg displayed diffuse positivity along with microvascular endothelial cells of peritubular capillaries, including thrombotic obstructions of such vessels (Fig. 1D). Thus circulating Plg seems to be retained inside the vasculature and probably gets activated by locally released tPA.

Experimental CC embolism induces thrombotic angiopathy, AKI and cortical necrosis

By selectively injecting CC into the left kidney artery, our model (Fig. 2A) avoids discomfort from skin ulcerations, peritonitis and uraemia, which would occur with diffuse CC embolism (Fig. 2B). Figure 2C illustrates the different segments of the intrarenal arteries. At 48 h after injection of 10 mg/kg CC, GFR decreased on average by 40%, i.e. AKI (Fig. 2D). The CC-exposed left kidney appeared swollen, with territorial discolorations, i.e. infarctions, compared with the unaffected contralateral kidney at 48 h (Fig. 2E). Histological analysis showed wide areas of cortical (and medullary) necrosis, interstitial oedema, loss of $CD31^+$ microvessels and neutrophil infiltrates lining the irregular shape of the territorial infarcts (Fig. 2F, Supplementary Fig. 3). Furthermore, we used SMA staining to localize interlobar, arcuate and interlobular arterial vessels and fibrin co-staining to localize clots surrounding CC clefts (Fig. 2F). Of note, the CC filled only a small part of the vascular lumen, while complete obstructions were exclusively observed in vessels filled with crystal-related clots. Thus experimental kidney CC embolism causes a diffuse thrombotic arteriopathy, AKI and ischaemic cortical necrosis with a perilesional inflammatory reaction known from territorial infarcts in other organs, such as myocardial infarction or ischaemic stroke [2, 10, 25, 26].

Time kinetics of crystal clot formation and growth

To characterize the temporal dynamics of crystal clot formation, we obtained kidneys at 2, 4, 6, 12, 18 and 48 h after CC injection (Fig. 3A). Although CCs were difficult to image directly in paraffin sections, as tissue processing with alcohols largely eliminates lipids, our previous studies demonstrated that arterial clots only form in proximity to CC impacted into the arterial vessels [9]. Nevertheless, we quantified the percentage of 'empty' arteries versus arteries

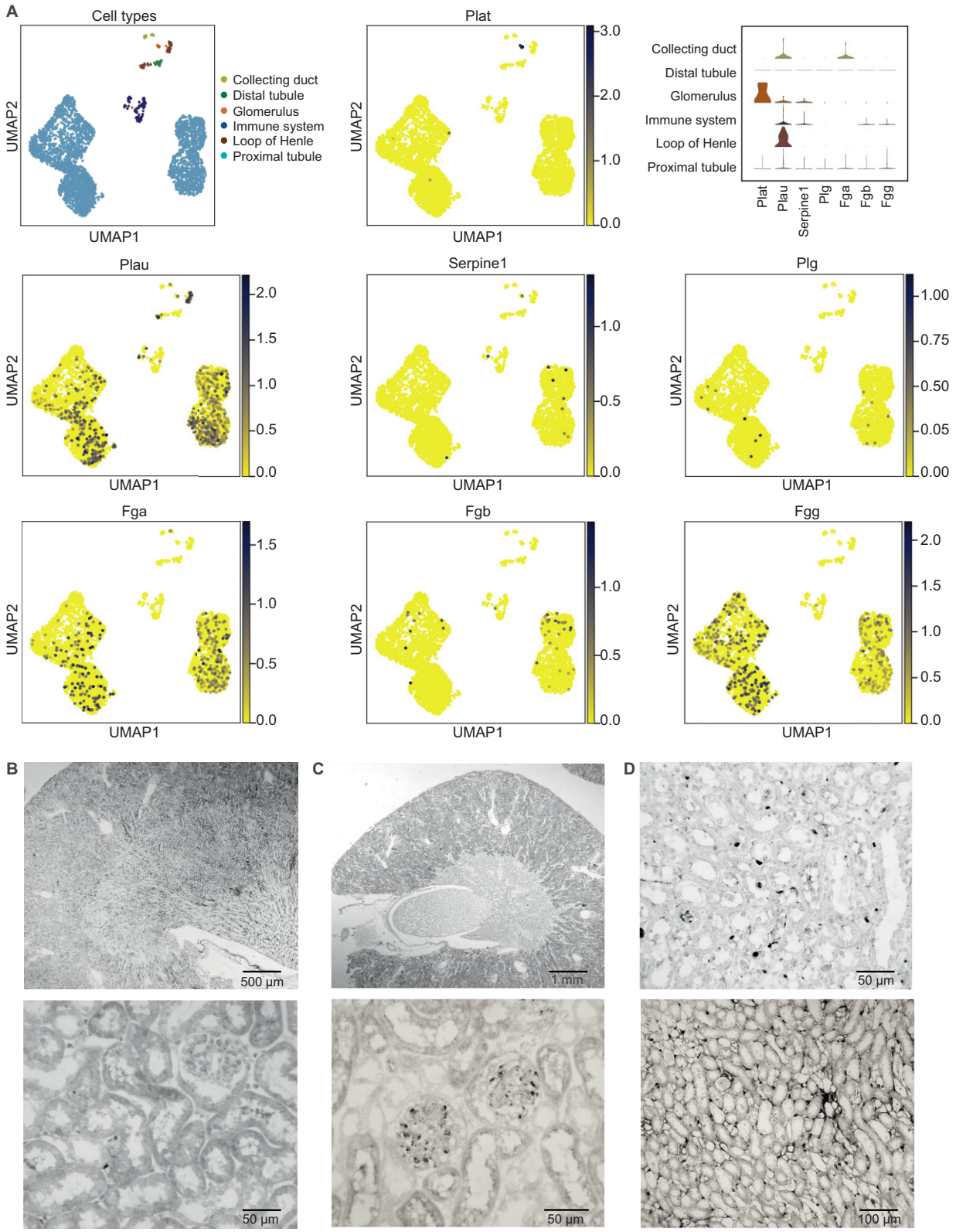

Figure 1: The expression of fibrinolytic factors in the mouse kidney. **(A)** UMAP plot showing the subclusters of cells of healthy mouse kidneys ($n = 4$) as defined by single-cell RNA sequencing. The annotation of cell types was performed as shown in Supplementary Fig. 1. The violin plots illustrate the quantitative expression levels for each gene per cluster as indicated. The dot blots show the cluster-specific expression of each of the depicted genes of the fibrinolytic system. Plat: tissue plasminogen activator; Plau: urokinase-type plasminogen activator; Serpine 1: plasminogen activator inhibitor-1; Plg: plasminogen; Fga, Fgb, Fgg: fibrinogen chain α, β and γ. **(B–D)** Immunostaining of healthy mouse kidney for **(B)** murine Plg and **(C)** tissue Plg activator tPA. Original magnifications 100× (left) and 400× (right). **(D)** Immunostaining of mouse kidney for human Plg after human Glu-Plg injection into healthy mice (left, original magnification 200×) or into mice with CC embolism (right, original magnification 200×). Scale bars as indicated.

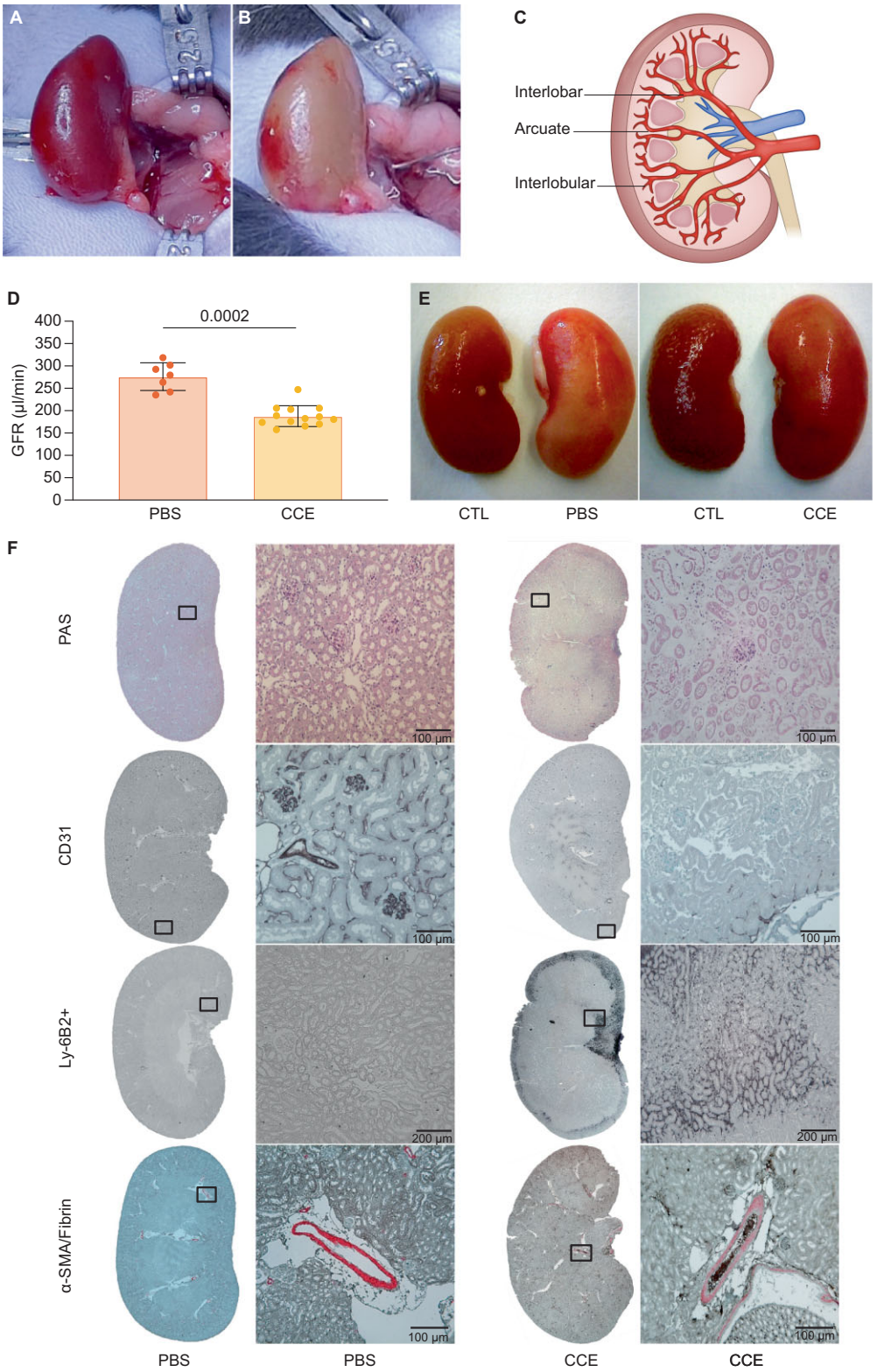

Figure 2: CC embolism induces thrombotic angiopathy, AKI and renal cortical necrosis. Illustrations of the surgical access to the injection site **(A)** before and **(B)** after intra-arterial injection of CCs. **(C)** Schematic of different kidney artery segments. **(D)** GFR at 48 h post-surgery of control mice without CC embolism and at 48 h with CC embolism. **(E)** Macroscopic appearance of both kidneys at 48 h post-intra-arterial injection (left kidney) with either saline or CC. Note the oedematous swelling of the kidney with CC embolism. **(F)** Representative images are shown for PAS staining, staining for $CD31^{+}$ endothelial cells to indicate healthy microvasculature, $Ly6G^{+}$ neutrophils to indicate the perilesional inflammatory reaction and fibrin-positive clots (black) in SMA-positive arteries (red) to indicate thrombotic angiopathy/crystal clots. All quantitative data are means ± standard error of the mean from 6–13 mice in each group. Scales bars indicate the original magnification in each panel.

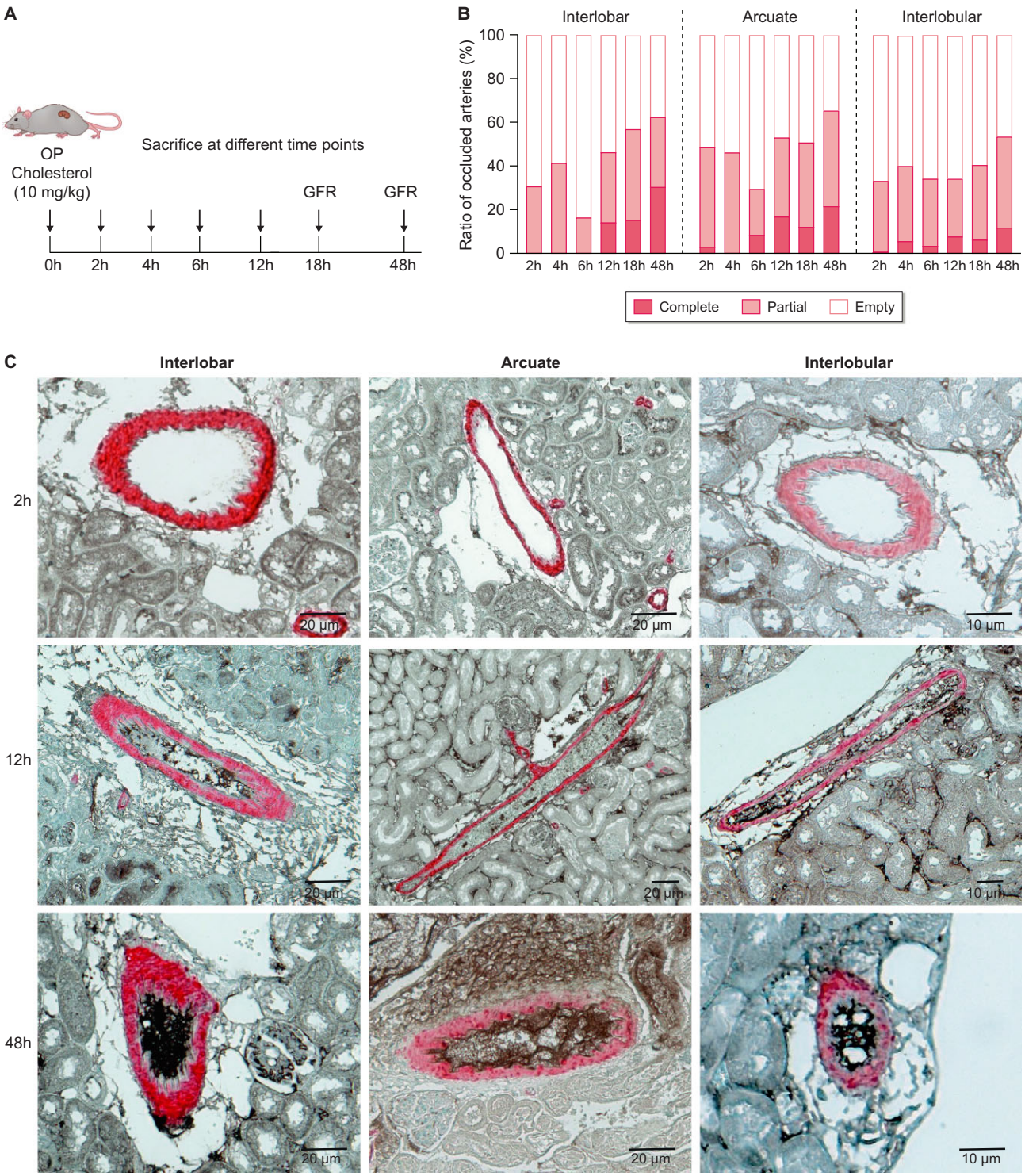

Figure 3: Time kinetics of crystal clot formation and growth. **(A)** Experimental design. **(B)** The quantitative assessment of thrombotic angiopathy is illustrated as the percentage of completely obstructed (complete: 100% of the lumen), partially obstructed (partial: 1–99%) or unobstructed (empty: 0%) in a separate analysis for interlobar, arcuate and interlobular arteries. Several time points of analysis after CC injection of 10 mg/kg are shown. All quantitative data derive from seven mice in each group. **(C)** Representative images are shown for some time points as fibrin-positive clots (black) in SMA-positive arteries (red). Scale bars indicate the original magnification in each panel.

affected by partial or complete obstructions. However, only complete obstructions could significantly impair glomerular perfusion of the respective nephrons, and hence GFR. Arterial thrombus formation initiated as early as 2 h after CC embolism and progressed with time so that the percentage of complete arterial occlusions increased with time as well (Fig. 3B, C). The progressively increasing complete arterial occlusions mechanistically should explain the decrease in GFR/AKI and the ischaemic necrosis seen at 48 h (Supplementary Fig. 3). These findings provided a rationale for delayed interventions that interfere with CC-induced thrombus growth.

Delayed intravenous Glu-Plg dose-dependently attenuates CC-induced thrombotic angiopathy

Human Glu-Plg extract could serve as an innovative therapeutic approach in the setting of CC embolism and offers advantages over other anticoagulants or fibrinolytic drugs within the aforementioned window of opportunity between CC embolism and complete vascular obstruction. We therefore injected different doses of Plg 4 h after CC injection and analysed GFR, crystal clots and kidney injury at 24 h, a time point where complete vascular obstructions had stably formed without any tendency towards resolution up to 48 h (Fig. 4A). With measured GFR as the prespecified primary endpoint, we noted an attenuation of GFR loss from baseline GFR with the highest efficacy at the highest dose, compared with control animals that had received the same injected volume of vehicle (Fig. 4B). Consistently and as a mechanistic explanation, Plg reduced the number of complete arterial obstructions by crystal clots with a corresponding effect on the number of arterial vessels affected by partial occlusions (Fig. 4C, D). This was associated with a corresponding reduction of ischaemic kidney injury, loss of $CD31^+$ microvasculature and the area of perilesional neutrophil infiltrates (Supplementary Fig. 4). Bleeding complications or tissue haemorrhages were not observed during the treatment period. Not even at the highest dose. Altogether, Plg therapy started hours after CC embolism can attenuate CC-induced thrombotic angiopathy, AKI and kidney cortical necrosis in a dose-dependent manner without increasing the risk of prolonged bleeding complications.

Intravenous Glu-Plg has a transient effect followed by crystal clot reappearance

Although we did not observe bleeding complications with even high-dose intravenous Plg, we further investigated if such an approach would be well-controllable, i.e. has only a transient thrombolytic effect before thrombus formation would again prevail. To assess this aspect, we chose an intermediate dose and assessed its effect on crystal clots at 4, 6, 12, 18, 24 and 48 h after intravenous injection (Fig. 5A). This dose of Plg transiently prevented crystal clot formation in the early phase (Fig. 5B, C). However, crystal clots started to grow with a delay of some hours and the total clot number progressively increased with time during the observation period. At 48 h, the total clot load was reduced compared with control mice of the same time point (Fig. 5B, C), but this did not affect the histological parameters of the injured kidney (Supplementary Fig. 5). This suggests that the effect of Plg therapy on the growth of crystal clots is transient, consistent with the concept of a dose-dependent effect on the local balance of thrombotic and thrombolytic factors. Thus we conclude that even delayed intravenous Plg has a dose-dependent protective effect on the development of crystal clots after CC embolism, which translates into the prevention of AKI and cortical necrosis of the kidney. This therapeutic effect is transient, which renders intravenous Plg well-controllable, e.g. in case (bleeding) complications occur. However, during the treatment period followed here, no haemorrhagic complications occurred. On the other hand, these data suggest that AKI and ischaemic infarction are best prevented with a higher dose of Plg and prolonged treatment, e.g. as done with platelet inhibitors in coronary artery thrombosis.

DISCUSSION

We hypothesized that human Glu-Plg could be a potential innovative drug candidate to attenuate the consequences of CC embolism, an otherwise severe complication of severe atherosclerosis that is frequently fatal in humans. Using a novel mouse model of experimental CC embolism we found that CC embolism induced a thrombotic angiopathy gradually progressing within 2–18 h in the interlobar, arcuate and interlobular arteries and leading to an increasing number of completely obstructed arteries followed by a decrease in GFR and ischaemic cortical necrosis; intravenous Plg started 4 h after CC embolism could attenuate crystal clot formation and prevent all the aforementioned features of the CC embolism syndrome, especially at the highest dose, without major bleeding complications; and Plg effects are transient, which might make Plg a well-controllable therapeutic option for patients with CC embolism at an acceptable safety profile.

We concluded earlier that not the CC alone, but CC clots, cause significant vascular obstructions, GFR loss and ischaemic cortical necrosis, because preventing clot formation, e.g. with heparin or DNase I, prevented GFR loss/AKI and kidney necrosis [9]. In addition, a GFR decrease is an immediate consequence of arterial obstruction, while cortical necrosis is more variable, and even completely preventing kidney necrosis does not prevent GFR loss/AKI as long as vascular obstructions remain unaffected [9]. Here we further explored the therapeutic window of crystal clot formation to determine the window of opportunity for innovative treatments of CC embolism syndrome–related AKI. CC embolism triggers crystal clot formation as early as after 2 h, because CC causes endothelial injury, the release of procoagulant factors from platelets and rapid complement activation *in vitro* [9, 27, 28]. The developing blood clots are composed of platelets, red and white blood cells, fibrin mesh and extracellular DNA that are released by damaged endothelial cells [29, 30]. The imbalanced coagulation system further enhances fibrinogenesis and the intrinsic fibrinolytic system could not attenuate thrombus growth and intravascular coagulation during CC embolism. Our results suggest that intravenous Plg could balance local fibrinolysis in the injured kidney arteries, thereby reducing

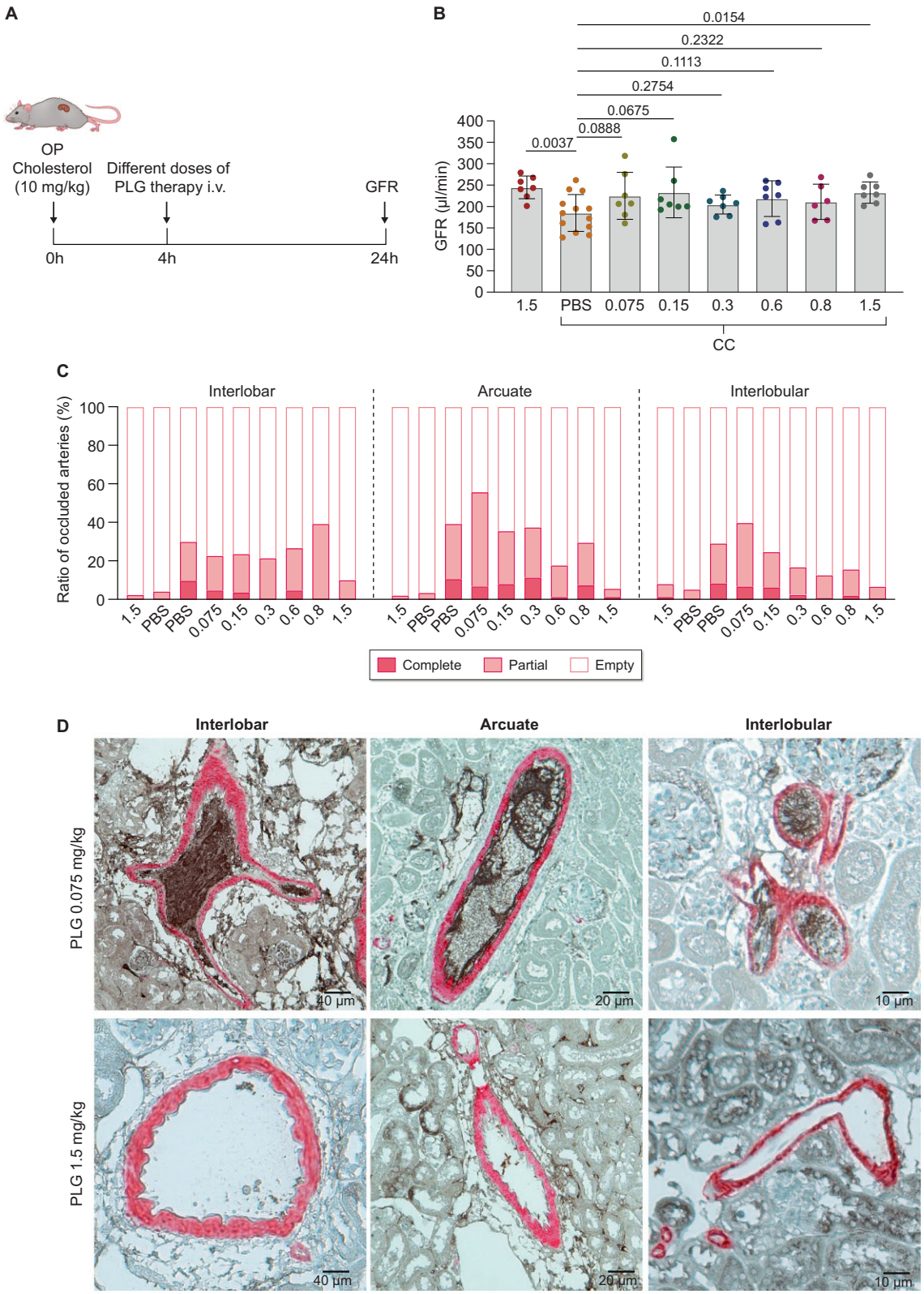

Figure 4: Plg therapy dose-dependently attenuates CC embolism syndrome. **(A)** Experimental design. **(B)** The GFR was measured before (left group) and 24 h after injection of CCs plus different doses of Plg, as indicated. **(C)** The quantitative assessment of thrombotic angiopathy is illustrated as the percentage of completely obstructed (complete: 100% of the lumen), partially obstructed (partial: 1–99%) or unobstructed (empty: 0%) in a separate analysis for interlobar, arcuate and interlobular arteries. Several time points of analysis after CC injection of 10 mg/kg are shown. All quantitative data derive from seven mice in each group. **(D)** Representative images are shown for selected dose groups as fibrin-positive clots (black) in SMA-positive arteries (red). Scale bars indicate the original magnification in each panel.

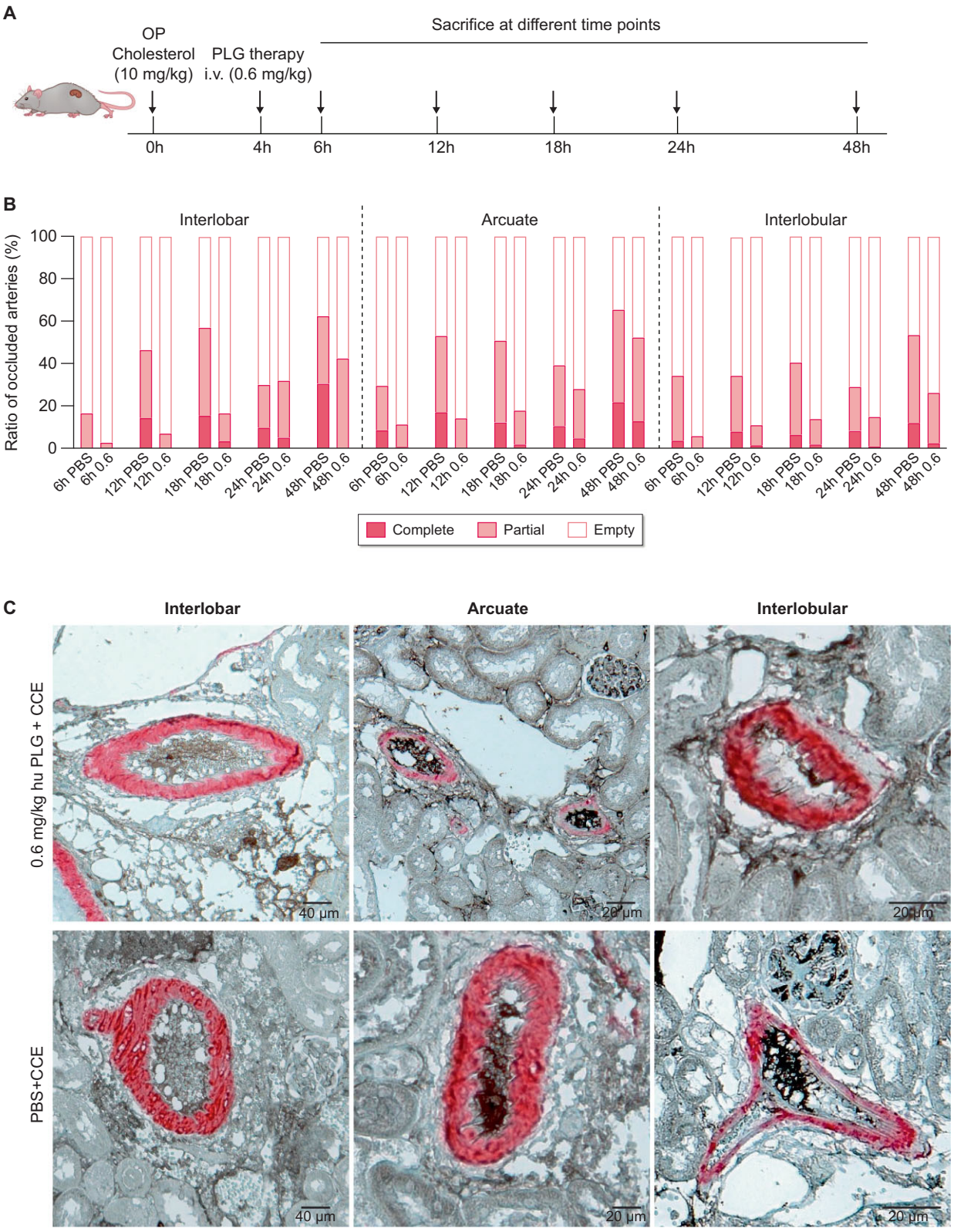

Figure 5: Plg has a transient fibrinolytic effect on crystal clot formation. **(A)** Experimental design. **(B)** The quantitative assessment of thrombotic angiopathy is illustrated as the percentage of completely obstructed (complete: 100% of the lumen), partially obstructed (partial: 1–99%) or unobstructed (empty: 0%) in a separate analysis for interlobar, arcuate and interlobular arteries. The graph summarizes obstructions at several time points after intravenous 0.6 mg/kg Glu-Plg 4 h after CC injection of 10 mg/kg. All quantitative data derive from seven mice in each group. **(C)** Representative images are shown for some time points as fibrin-positive clots (black) in SMA-positive arteries (red). Scales bars indicate the original magnification in each panel.

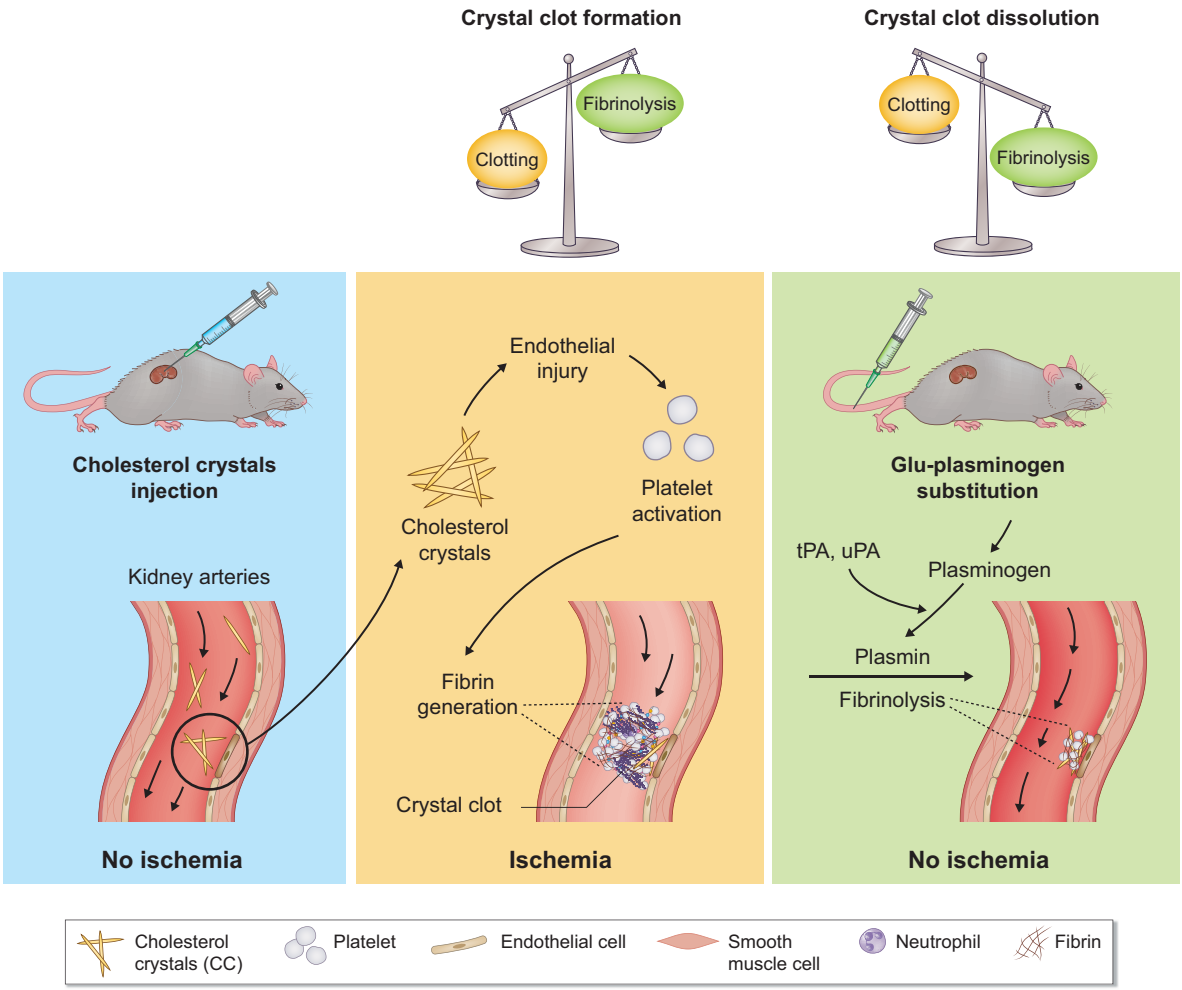

Figure 6: Schematic illustration of the putative mechanism of action of Glu-Plg therapy in CC embolism. (Left panel) We induced CC embolism syndrome by injecting CC into the kidney artery of mice to avoid painful tissue necrosis in other organs. (Middle panel) CC getting stuck in intrarenal arteries induced endothelial injury, platelet activation, fibrin generation and local crystal clot formation. This process likely involves the fibrinolytic system, but the predominance of clotting factors leads to progressive arterial thrombosis. Crystal clots completely obstructing the lumen of pre-glomerular arterial vessels leads to a decrease in GFR and ischaemic cortical necrosis (not shown). (Right panel) Intravenous Glu-Plg substitutes the consumption of local Plg, a substrate to tPA or urokinase-type-plasminogen activator (uPA) for the generation of plasmin, the central enzyme of the fibrinolytic system that can degrade the fibrin mesh. Hence intravenous Glu-Plg can limit the growth and even dismantle crystal clots, which can reduce the number of completely obstructed intrarenal arteries, sustain GFR and prevent tissue necrosis in CC embolism.

fibrin mesh and blood clot formation (Fig. 6). However, limitations of our study include the short time point of the analysis. Therefore we cannot exclude that continuous anticoagulant therapy may be necessary to prevent recurrent crystal clot formation. Furthermore, animal welfare considerations did not allow us to perform bilateral CC embolism in mice, thus we only studied unilateral CC embolism, which is not such a concern in the clinical practice of humans. Our study with human Plg in mice may trigger cross-species interactions. However, results with human Plg used in our experiments may be further explored for potential clinical application in a dedicated clinical development program.

Streptokinase, tPA and urokinase are potent fibrinolytic drugs in clinical use that can dissolve arterial (and venous) thrombi [15], as previously demonstrated for urokinase in our CC embolism model [9], but such intervention can cause bleeding complications in humans and mice [31]. Intravenous human Glu-Plg could represent a possible solution to interfere with fibrin formation at the site of thrombus growth without strongly affecting haemostasis [30, 31]. Indeed, our data show a dose-dependent effect of Plg on arterial thrombus growth, AKI and kidney infarction without affecting primary haemostasis. The effect of Plg on the growth of crystal clots was transient and corresponded to the reversible pharmacodynamics of anticoagulants or fibrinolytic drugs in clinical use [15]. Therefore we do not attribute the lack of bleeding complications to the transient activity of Plg, but rather to its different biological role as a substrate for plasmin formation. This leaves the control of the fibrinolytic process to the local balance of Plg activators versus their inhibitors rather than overruling this balance as it occurs with urokinase, streptokinase or tPA therapy [15, 16, 32]. Thus intravenous

Plg may be a safer way to attenuate crystal clot formation, especially in the complex clinical settings of patients with CC embolism.

Interestingly, Plg also elicits renoprotective effects in experimental models of glomerulonephritis [33, 34].

Human Glu-Plg therapy can attenuate thrombotic angiopathy, GFR loss/AKI and cortical necrosis in a dose-dependent manner even if started 4 h after CC embolism occurred. As with other anticoagulants, the thrombolytic effects are transient, but in contrast to our previous experience with urokinase in this model, no bleeding complications occurred with Plg. These data suggest that intravenous Plg could be a potential therapeutic approach in patients with CC embolism syndrome.

SUPPLEMENTARY DATA

Supplementary data are available at *ndt* online.

FUNDING

This study was supported by a research grant from PreviPharma (to Y.L.). S.C., L.Y. and Y.L. received support from the Chinese Scholarship Council. H.J.A. was supported by the Deutsche Forschungsgemeinschaft (AN372/16-2, 20-2, 30-1).

AUTHORS' CONTRIBUTIONS

R.W. and S.T.K. purified Glu-Plg from human plasma. H.J.A. and S.K.D. designed the study. L.L., S.C. and D.Z. performed the animal experiments. L.D.C., R.S., S.L. and P.R. performed single-cell RNA sequencing analysis. Y.L., L.Y, S.K.D. and E.M.B. performed tissue and image analysis. Y.L. and H.J.A. secured funding. L.L., Y.L., S.C., E.M.B. and H.J.A. drafted the first version of the manuscript. All authors edited and approved the final version of the manuscript.

DATA AVAILABILITY STATEMENT

The data underlying this article are available in the article and in its online supplementary material.

CONFLICT OF INTEREST STATEMENT

S.K.D., R.W. and S.K. are employees of PreviPharma. Y.L. received a research grant from PreviPharma. H.J.A. received consultancy fees from PreviPharma.

REFERENCES

1. Weber C, Noels H. Atherosclerosis: current pathogenesis and therapeutic options. *Nat Med* 2011;**17**:1410–22. http://dx.doi.org/10.1038/nm.2538.
2. Frangogiannis NG. Pathophysiology of myocardial infarction. *Compr Physiol* 2015;**5**:1841–75. http://dx.doi.org/10.1002/cphy.c150006.
3. Scolari F, Ravani P. Atheroembolic renal disease. *Lancet* 2010;**375**:1650–60. http://dx.doi.org/10.1016/S0140-6736(09)62073-0.
4. Moolenaar W, Lamers CB. Cholesterol crystal embolization in the Netherlands. *Arch Intern Med* 1996;**156**:653–7. http://dx.doi.org/10.1001/archinte.1996.00440060081009.
5. Agrawal A, Ziccardi MR, Witzke C *et al.* Cholesterol embolization syndrome: an under-recognized entity in cardiovascular interventions. *J Interv Cardiol* 2018;**31**:407–15. http://dx.doi.org/10.1111/joic.12483.
6. Thadhani RI, Camargo CA, Jr, Xavier RJ *et al.* Atheroembolic renal failure after invasive procedures. Natural history based on 52 histologically proven cases. *Medicine (Baltimore)* 1995;**74**:350–8. http://dx.doi.org/10.1097/00005792-199511000-00005.
7. Li X, Bayliss G, Zhuang S. Cholesterol crystal embolism and chronic kidney disease. *Int J Mol Sci* 2017;**18**:1120.
8. Meyrier A. Cholesterol crystal embolism: diagnosis and treatment. *Kidney Int* 2006;**69**:1308–12. http://dx.doi.org/10.1038/sj.ki.5000263.
9. Shi C, Kim T, Steiger S *et al.* Crystal clots as therapeutic target in cholesterol crystal embolism. *Circ Res* 2020;**126**:e37–52. http://dx.doi.org/10.1161/CIRCRESAHA.119.315625.
10. Diethelm A, Vorburger C, Anabitarte M *et al.* [Cholesterol crystal embolisms due to systemic thrombolysis of an acute myocardial infarct]. *Schweiz Med Wochenschr* 1994;**124**:1437–41. https://www.ncbi.nlm.nih.gov/pubmed/7939511.
11. Lekeufack JB, Delrée P, Goergen M *et al.* [Multiple cholesterol emboli syndrome: beneficial effects of early heparin therapy. A case report]. *Ann Cardiol Angeiol (Paris)* 1999;**48**:575–8. https://www.ncbi.nlm.nih.gov/pubmed/12555463.
12. Wakabayashi T, Yoshizawa Y, Kawana S. Successful use of heparin and warfarin in the treatment of cholesterol crystal embolization. *J Dermatol* 2008;**35**:111–4. http://dx.doi.org/10.1111/j.1346-8138.2008.00425.x.
13. Allingstrup M, Wetterslev J, Ravn FB *et al.* Antithrombin III for critically ill patients. *Cochrane Database Syst Rev* 2016;**2**:CD005370. https://www.ncbi.nlm.nih.gov/pubmed/26858174.
14. Bernard GR, Vincent JL, Laterre PF *et al.* Efficacy and safety of recombinant human activated protein C for severe sepsis. *N Engl J Med* 2001;**344**:699–709. http://dx.doi.org/10.1056/NEJM200103083441001.
15. Kumar SS, Sabu A. Fibrinolytic enzymes for thrombolytic therapy. *Adv Exp Med Biol* 2019;**1148**:345–81. http://dx.doi.org/10.1007/978-981-13-7709-9_15.
16. Kwaan HC. From fibrinolysis to the plasminogen-plasmin system and beyond: a remarkable growth of knowledge, with personal observations on the history of fibrinolysis. *Semin Thromb Hemost* 2014;**40**:585–91. https://www.ncbi.nlm.nih.gov/pubmed/25000957.
17. Sakharov DV, Rijken DC. Superficial accumulation of plasminogen during plasma clot lysis. *Circulation* 1995;**92**:1883–90. http://dx.doi.org/10.1161/01.CIR.92.7.1883.
18. Marschner JA, Schäfer H, Holderied A *et al.* Optimizing mouse surgery with online rectal temperature monitoring and preoperative heat supply. Effects on post-ischemic acute kidney injury. *PLoS One* 2016;**11**:e0149489. http://dx.doi.org/10.1371/journal.pone.0149489.
19. Dobin A, Davis CA, Schlesinger F *et al.* STAR: ultrafast universal RNA-seq aligner. *Bioinformatics* 2013;**29**:15–21. http://dx.doi.org/10.1093/bioinformatics/bts635.
20. Lun AT, McCarthy DJ, Marioni JC. A step-by-step workflow for low-level analysis of single-cell RNA-seq data with Bioconductor. *F1000Research* 2016;**5**:2122.
21. McInnes L, Healy J, Melville J. UMAP: Uniform manifold approximation and projection for dimension reduction. https://arxiv.org/abs/1802.03426 (2 October 2022, date last accessed).
22. Mulay SR, Thomasova D, Ryu M *et al.* MDM2 (murine double minute-2) links inflammation and tubular cell healing during acute kidney injury in mice. *Kidney Int* 2012;**81**:1199–211. http://dx.doi.org/10.1038/ki.2011.482.
23. Stallone G, Pontrelli P, Rascio F *et al.* Coagulation and fibrinolysis in kidney graft rejection. *Front Immunol* 2020;**11**:1807. http://dx.doi.org/10.3389/fimmu.2020.01807.
24. Svenningsen P, Hinrichs GR, Zachar R *et al.* Physiology and pathophysiology of the plasminogen system in the kidney. *Pflugers Arch* 2017;**469**:1415–23. http://dx.doi.org/10.1007/s00424-017-2014-y.
25. Laridan E, Denorme F, Desender L *et al.* Neutrophil extracellular traps in ischemic stroke thrombi. *Ann Neurol* 2017;**82**:223–32. http://dx.doi.org/10.1002/ana.24993.
26. Orellana-Urzúa S, Rojas I, Líbano L *et al.* Pathophysiology of ischemic stroke: role of oxidative stress. *Curr Pharm Des* 2020;**26**:4246–60. http://dx.doi.org/10.2174/1381612826666200708133912.

27. Falasca GF, Ramachandrula A, Kelley KA *et al.* Superoxide anion production and phagocytosis of crystals by cultured endothelial cells. *Arthritis Rheum* 1993;**36**:105–16. http://dx.doi.org/10.1002/art.1780360118.
28. Nymo S, Niyonzima N, Espevik T *et al.* Cholesterol crystal-induced endothelial cell activation is complement-dependent and mediated by TNF. *Immunobiology* 2014;**219**:786–92. http://dx.doi.org/10.1016/j.imbio.2014.06.006.
29. Engelmann B, Massberg S. Thrombosis as an intravascular effector of innate immunity. *Nat Rev Immunol* 2013;**13**:34–45. http://dx.doi.org/10.1038/nri3345.
30. Mackman N. Triggers, targets and treatments for thrombosis. *Nature* 2008;**451**:914–8. http://dx.doi.org/10.1038/nature06797.
31. Kluft C, Sidelmann JJ, Gram JB. Assessing safety of thrombolytic therapy. *Semin Thromb Hemost* 2017;**43**:300–10. https://www.ncbi.nlm.nih.gov/pubmed/27272963.
32. Mukhopadhyay S, Johnson TA, Duru N *et al.* Fibrinolysis and inflammation in venous thrombus resolution. *Front Immunol* 2019;**10**:1348. http://dx.doi.org/10.3389/fimmu.2019.01348.
33. Kitching AR, Holdsworth SR, Ploplis VA *et al.* Plasminogen and plasminogen activators protect against renal injury in crescentic glomerulonephritis. *J Exp Med* 1997;**185**:963–8. http://dx.doi.org/10.1084/jem.185.5.963.
34. Malliaros J, Holdsworth SR, Wojta J *et al.* Glomerular fibrinolytic activity in anti-GBM glomerulonephritis in rabbits. *Kidney Int* 1993;**44**:557–64. http://dx.doi.org/10.1038/ki.1993.281.

Received: 21.4.2022; Editorial decision: 1.9.2022